J. Fluid Mech. (1980), *vol.* 100, *part* 4, *pp.* 785–800
Printed in Great Britain

Weld-pool sag

By J. G. ANDREWS, D. R. ATTHEY
CEGB, Marchwood Engineering Laboratories,
Southampton S04 4ZB
AND J. G. BYATT-SMITH
Department of Mathematics, Kings Buildings,
University of Edinburgh

(Received 15 October 1977 and in revised form 23 February 1980)

The shape of the liquid/gas interface of a weld pool is determined by the balance of gravitational and surface tension forces. Equilibrium profiles and stability criteria are derived for vertical and horizontal situations.

1. Introduction

In many welding situations the orientation of the workpiece may be such that the liquid metal in the weld pool will tend to sag under gravity. A restoring mechanism is surface tension and the eventual shape of the liquid/air (or shielding gas) profile is the result of a balance between gravitational and surface-tension forces. In this paper we consider a variety of problems, based on vertical and horizontal specimens, and look for equilibrium profiles and stability criteria.

The shapes of the solidified welds are of practical importance. The shape of penetrating beads affects the fatigue properties of welded joints and is of particular significance in boiler plant (since the through-flow of fluids may be disturbed by excessive weld-bead protrusions). In nuclear plant the tolerance for unfavourable contours may be much less owing to the risk of downstream accumulation of debris which may give rise to corrosion or erosion hazards in high heat-flux designs. The loss of total section would also be unacceptable and is sometimes difficult to monitor. Currently there is almost total reliance on welding procedure and manufacturing fit-up parameters to obtain suitable weld-bead contours, so there is a strong motivation to examine by theoretical models the predicted shape of such contours and to determine the main controlling parameters.

The subject of equilibrium and stability of hanging liquid drops has been re-opened in recent years by Padday (1971), Padday & Pitt (1973), Pitts (1973, 1974, 1976) and Majumdar & Michael (1976), who considered the problem of a water droplet suspended from a horizontal plane or tap. Some work more directly related to welding has been carried out by Nishiguchi, Ohji & Matsui (1977) on the shape of liquid weld metal when welding an L-shaped joint with the use of filler metal. J. C. Meewezen (1976, private communication) has done some experiments on welding vertical tubes without the addition of filler metal under a variety of conditions. A few of his photographs of sections of the solidified profile are presented here.

The aim of this paper is to model the shapes of the free surfaces in the important

0022–1120/80/4560–2250 $02.00

cases of welding vertical and horizontal plates. The main simplifying assumptions that we make are the neglect of fluid motion, uniformity of arc pressure and of surface-tension coefficient. We also idealize the geometry by considering only two-dimensional situations. In addition we consider the question of whether our equilibrium profiles are stable.

It is important to note that throughout this work we consider solid and liquid regions which are different phases of the same material. This means that the interface between the two phases will not be sharply defined. In practice there is a region which contains both solid and liquid material in thermodynamic equilibrium and which is typically tens of micrometres in thickness. This is in contrast to the usual surface-tension problems of different materials in contact, where the transition region will be only a few atomic layers in thickness. Hence it is no longer appropriate to think in terms of a unique contact angle and instead it is more reasonable to apply a boundary condition of attachment at the corner of the liquid region.

2. Vertical plate

2.1. *One-sided two-dimensional profile*

We consider a vertical surface of a thick block of material which is being heated locally by a surface heat source so as to form a weld pool. Owing to gravity, the molten metal sags and may be supported by surface tension. In this section we assume that the material does not melt through to the other side. It is assumed that the pool is infinite in the third (namely z) direction.

Ignoring fluid flow in the pool, the total potential energy per unit length in the z direction is

$$\int_{-\frac{1}{2}L}^{\frac{1}{2}L} \left(T\frac{ds}{dx} - \rho g x y\right) dx, \tag{1}$$

taking LT as the energy of the undistorted surface, where $s(x)$ is the length of surface measured from the top of the pool ($x = -\frac{1}{2}L$), T is the coefficient of surface tension, ρ is the density of the material and g is the acceleration due to gravity. We initially restrict our attention to profiles which lie entirely in the range $-\frac{1}{2}L \leqslant x \leqslant L$; the overhanging case is considered later in this section. The equilibrium profile must be that surface $y(x)$ which minimizes the total potential energy, E, subject to the constraint of mass conservation (assuming that no liquid is lost)

$$\int_{-\frac{1}{2}L}^{\frac{1}{2}L} y\,dx = 0. \tag{2}$$

The boundary conditions we apply are that the free surface remains attached to the corners, so that $y = 0$ at both $x = -\frac{1}{2}L$ and $x = \frac{1}{2}L$. Putting

$$F = T\,ds/dx - \rho g x y - \lambda y,$$

where $ds/dx = (1+y'^2)^{\frac{1}{2}}$ and λ is the Lagrange multiplier, in the Euler–Lagrange formula for the equilibrium shape

$$\partial F/\partial y - (d/dx)(\partial F/\partial y') = 0$$

(Craggs 1973), we immediately obtain the differential equation

$$T\frac{d}{dx}[(dy/dx)/\{1+(dy/dx)^2\}^{\frac{1}{2}}] = -\rho g(x-c), \tag{3}$$

where $c = -\lambda/\rho g$ is a constant, unknown at this stage of the calculation. This arbitrariness arises because we do not have any reference point for pressure inside the liquid.

We introduce the following normalized variables

$$X = x/L, \quad Y = y/L, \quad C = c/L, \quad \epsilon = \rho g L^2/T. \tag{4}$$

Equation (3) becomes

$$\{Y'/(1+Y'^2)^{\frac{1}{2}}\}' = -\epsilon(X-C), \tag{5}$$

where the prime refers to d/dX.

Integrating once, we obtain

$$Y'/(1+Y'^2)^{\frac{1}{2}} = -\epsilon(\tfrac{1}{2}X^2 - CX - K^2), \tag{6}$$

where we have written the constant of integration as $-K^2$. We will show below that K must be real. Equation (6) must be solved together with the constraint (2), which we write in non-dimensional form

$$\int_{-\frac{1}{2}}^{\frac{1}{2}} Y\,dX = 0. \tag{7}$$

Putting $f(X) = \frac{1}{2}X^2 - CX - K^2$ in equation (6) and rearranging gives

$$Y' = -\epsilon f/(1-\epsilon^2 f^2)^{\frac{1}{2}}, \tag{8}$$

where we have taken the negative sign in the square root for self-consistency.

We can readily show that the profile has a point of inflexion at the centre $X = 0$ by the following argument. Integrating (7) by parts, using the boundary conditions $Y = 0$ at $X = \pm\frac{1}{2}$, we have

$$\int_{-\frac{1}{2}}^{\frac{1}{2}} Y'(X-C)\,dX = 0.$$

Writing $f' = X - C$ and substituting in the above integral yields

$$\int_{-\frac{1}{2}}^{\frac{1}{2}} ff'(1-\epsilon^2 f^2)^{-\frac{1}{2}}\,dX = 0$$

or

$$[(1-\epsilon^2 f^2)^{\frac{1}{2}}]_{-\frac{1}{2}}^{\frac{1}{2}} = 0,$$

from which we find $C = 0$ and hence note from equation (5) that the curvature is zero at $X = 0$. (The other solution, with $K^2 = \frac{1}{8}$ and C arbitrary, can be shown to contradict the mass conservation condition (7).) Furthermore, Y' is symmetric about $X = 0$ from equation (6) and in view of the boundary conditions $Y = 0$ at $X = \pm\frac{1}{2}$ it follows that $Y(X)$ is antisymmetric about $X = 0$.

Substituting $f = \frac{1}{2}X^2 - K^2$ into equation (8) gives†

$$Y' = -\epsilon(\tfrac{1}{2}X^2 - K^2)/\{1-\epsilon^2(\tfrac{1}{2}X^2 - K^2)^2\}^{\frac{1}{2}}. \tag{9}$$

Noting that K has to be real for Y' to be zero somewhere in the range $-\frac{1}{2} \leqslant X \leqslant \frac{1}{2}$, making the substitutions

$$\xi = X/(2^{\frac{1}{2}}K), \quad \mu = \epsilon K^2$$

and integrating yields

$$Y(\xi) = 2^{\frac{1}{2}}\mu K \int_0^{\xi} \frac{(1-\xi^2)\,d\xi}{\{1-\mu^2(1-\xi^2)^2\}^{\frac{1}{2}}}. \tag{10}$$

For computational purposes, it is convenient to express this integral in terms of elliptic integrals in the form

$$Y(\xi) = (-K/\mu^{\frac{1}{2}})\,[2\{E(\tfrac{1}{2}\pi \mid m) - E(\phi \mid m)\} - \{F(\tfrac{1}{2}\pi \mid m) - F(\phi \mid m)\}], \tag{11}$$

where E and F are the elliptic integrals of the second and first kind, respectively, $\xi = (1+1/\mu)^{\frac{1}{2}}\cos\phi$ and $m = \frac{1}{2}(1+\mu)$.

The boundary condition $Y = 0$ at $X = \frac{1}{2}$ may now be applied to determine K. Figure 1 shows the profiles for various values of the dimensionless surface-tension parameter ϵ. For small ϵ the linearized solution

$$Y(X) = \tfrac{1}{6}\epsilon X(\tfrac{1}{4} - X^2)$$

corresponding to $K = 1/\sqrt{24}$ is a good approximation. For larger ϵ the curvature increases and nonlinear effects are clearly important. There is a value of ϵ, $\epsilon = \epsilon_1$ say, for which the profile becomes horizontal at the corners, i.e. $Y' \to \infty$. This value may be determined by noting that the denominator of equation (9) must be zero for $X = \pm\frac{1}{2}$.

For $\epsilon > \epsilon_1$, we must integrate through the square-root singularity in the integral (10) and provided we take the correct sign for Y' everywhere we obtain a double-valued profile which overhangs the corner $X = \frac{1}{2}$. The equation of the profile is still given by (11), which may now be regarded as giving the profile in terms of the parameter ϕ. As ϕ decreases from $\frac{1}{2}\pi$ to 0, the profile is traced out from the point of inflexion $X = 0$ to the point $X = X_{\max}$, where the tangent is horizontal. The remainder of the profile from $X = X_{\max}$ to $X = \frac{1}{2}$ corresponds to negative values of ϕ.

As we increase the value of μ from $\mu = 0{\cdot}65\ldots$, which corresponds to $\epsilon = \epsilon_1 = 13{\cdot}21\ldots$ to $\mu = 0{\cdot}70\ldots$, which corresponds to $\epsilon = \epsilon_2 = 13{\cdot}46\ldots$, we trace out a sequence of overhanging profiles. Increasing μ still further, we are able to obtain new overhanging profiles with ϵ decreasing from $\epsilon = \epsilon_2$. A limiting profile is reached for $\epsilon = \epsilon_3 = 6{\cdot}82\ldots$, $\mu = 0{\cdot}85\ldots$, which has a vertical tangent at the point of contact $X = \frac{1}{2}$. No profiles exist for $\mu > 0{\cdot}85$. It is possible to obtain overhanging profiles for $\epsilon < \epsilon_3$, with μ decreasing from $0{\cdot}85$ as ϵ decreases; however these profiles must be rejected on physical grounds as they would have liquid metal in the region $X > \frac{1}{2}$, $Y < 0$, which we have assumed to be solid. Figure 2 shows overhanging profiles for several values of ϵ and figure 3 shows the variation of K with ϵ. From figure 3 we see that three cases can arise.

† The derivation of (9) only applies to single-valued weld profiles. Overhanging profiles may be considered in terms of a parameter which varies monotonically along the length of the profile. This approach leads to an equation which is identical with (9), except that the sign of Y' changes as we move through the lowest point of the profile.

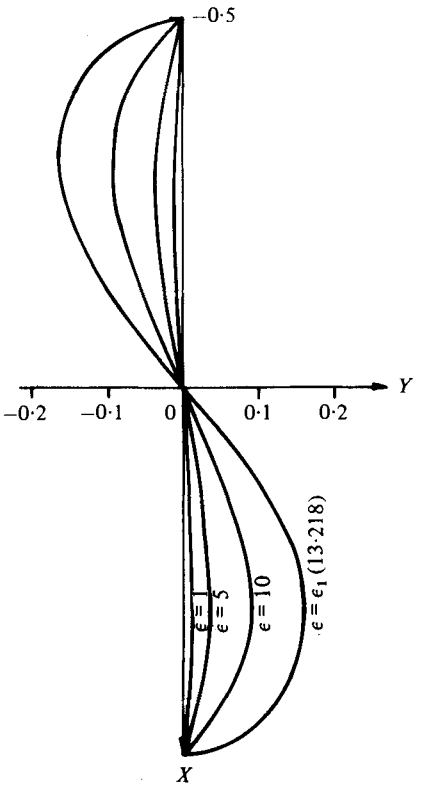

FIGURE 1. Equilibrium profiles for a two-dimensional vertical weld for various values of the parameter $\epsilon = \rho g L^2/T$.

For $\epsilon < \epsilon_3$ there is a unique profile which is single-valued. For $\epsilon_3 < \epsilon < \epsilon_1$, there is one overhanging profile and one single-valued profile, while for $\epsilon_1 < \epsilon < \epsilon_2$ there are two overhanging profiles.

2.2. *Two-sided two-dimensional profile*

We may readily extend the model to the case where the molten zone penetrates right through the material so that there are two free surfaces, $y_1(x)$ and $y_2(x)$, to be determined. Furthermore, we can allow for a pressure drop, Δp, between the two sides. The equations for the two surfaces are of the same form as equation (5) for the one-sided problem, i.e.

$$\{Y_1'(1+Y_1'^2)^{-\frac{1}{2}}\}' = -\epsilon(X-C)+\Delta P \tag{12}$$

and

$$\{Y_2'(1+Y_2'^2)^{-\frac{1}{2}}\}' = \epsilon(X-C), \tag{13}$$

where

$$Y_1 = y_1/L_1, \quad Y_2 = y_2/L_1, \quad X = x/L_1, \quad \epsilon = \rho g L_1^2/T, \quad \Delta P = L_1 \Delta p/T, \tag{14}$$

where L_1 and L_2 are the front and back widths, respectively, and C is some arbitrary constant. Mass conservation relates the two surfaces by the condition

$$\int_{-\frac{1}{2}}^{\frac{1}{2}} Y_1 dX - \int_{-\frac{1}{2}\lambda}^{\frac{1}{2}\lambda} Y_2 dX = 0, \tag{15}$$

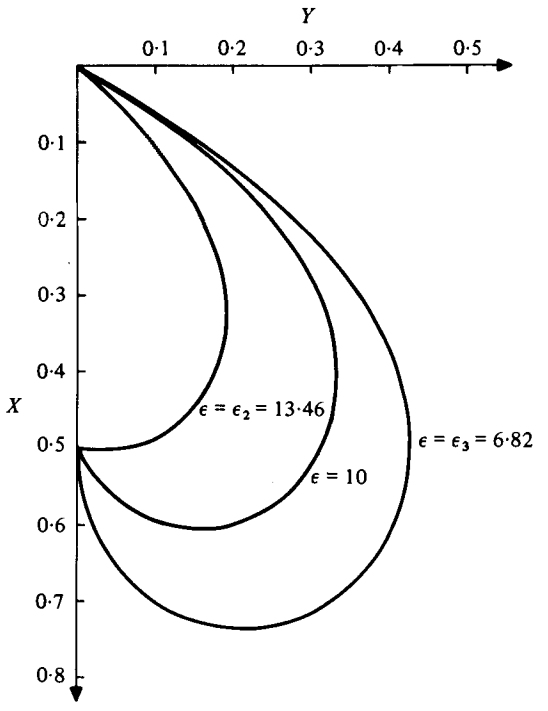

FIGURE 2. Overhanging equilibrium profiles (lower half only) for a two-dimensional vertical weld.

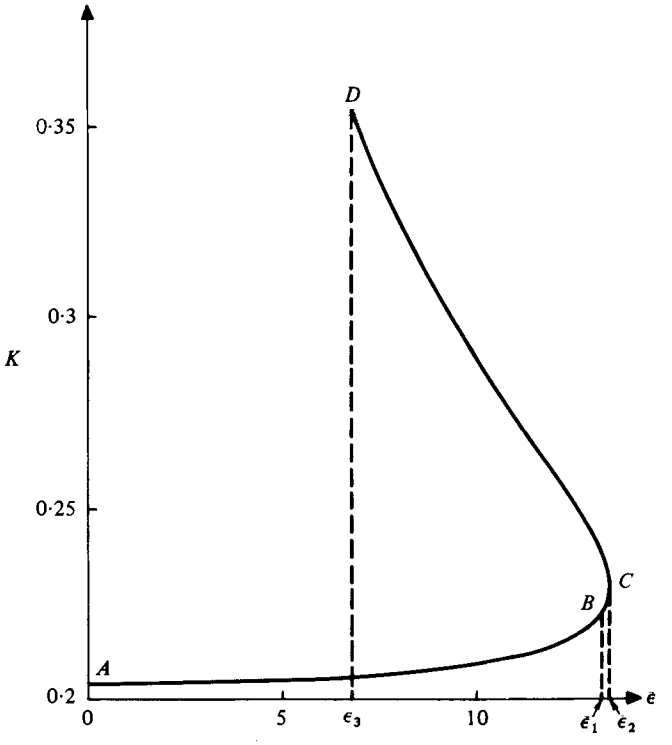

FIGURE 3. Variation of ϵ with K for one-sided vertical profiles.

where $\lambda = L_2/L_1$ and the planes $Y_1 = 0$ and $Y_2 = 0$ are taken to be the undistorted surfaces of the plate. Integrating (12) and (13) once, and rearranging, gives

$$Y_1' = -\epsilon f_1/(1-\epsilon^2 f_1^2)^{\frac{1}{2}} \tag{16}$$

and

$$Y_2' = \epsilon f_2/(1-\epsilon^2 f_2^2)^{\frac{1}{2}}, \tag{17}$$

where

$$f_1(X) = \tfrac{1}{2}X^2 - (C + \Delta P/\epsilon)\,X - K_1, \tag{18}$$

$$f_2(X) = \tfrac{1}{2}X^2 - CX - K_2, \tag{19}$$

and K_1 and K_2 are constants of integration.

Following the same lines as in § 2.1, we can express the mass conservation equation (15) in terms of f_1 and f_2, viz.

$$[1-\epsilon^2 f_1^2(\tfrac{1}{2})]^{\frac{1}{2}} - [1-\epsilon^2 f_1^2(-\tfrac{1}{2})]^{\frac{1}{2}} + [1-\epsilon^2 f_2^2(\tfrac{1}{2}\lambda)]^{\frac{1}{2}} - [1-\epsilon^2 f_2^2(-\tfrac{1}{2}\lambda)]^{\frac{1}{2}} = 0, \tag{20}$$

using the attachment conditions $Y_1 = 0$ at $X = \pm\frac{1}{2}$ and $Y_2 = 0$ at $X = \pm\frac{1}{2}\lambda$. Integrating equation (16) from $X = -\frac{1}{2}$ to $X = \frac{1}{2}$ yields

$$\int_{-\frac{1}{2}}^{\frac{1}{2}} f_1(1-\epsilon^2 f_1^2)^{-\frac{1}{2}}\,dX = 0,$$

which may be reduced to elliptic integrals by standard methods. Equation (17) may be treated in a similar way, which together with equation (20) gives three nonlinear equations in the three unknowns C, K_1 and K_2.

When $\Delta P = 0$, we find that $C = 0$ and the problem decouples, both surfaces being the solution of the appropriate one-sided problem. When a pressure drop is applied across the plate, the surfaces tend to bulge towards the side at lower pressure as shown in figure 4. As for the one-sided problem, solutions exist which overhang on either the front or the back faces and a limit arises when either surface becomes vertical at a corner. Beyond this limit a steady solution does not exist.

As might be expected, the pressure drop required to produce this critical condition is very small; typically it is around 1% atmospheric pressure. Hence we note that the weld profiles must be very sensitive to any variation in pressure, which might be caused by shielding gas, outgassing, arc pressure or side draughts.

2.3. *Stability for vertical slot*

It is clearly important to establish whether the equilibrium profiles we have obtained are actually stable. We first consider the simplest problem of § 2.1 and we restrict our attention to disturbances which leave the problem two-dimensional. From (1), the total potential energy per unit length, scaled by the factor LT, is

$$E = \int_{-\frac{1}{2}}^{\frac{1}{2}} \{(1+Y'^2)^{\frac{1}{2}} - \epsilon X Y\}\,dX.$$

We shall first show that the profiles corresponding to the segment AB on figure 3 (i.e. the single-valued profiles) are stable. Suppose that the shape of the surface is distorted slightly from its equilibrium value $Y(X)$ to $Y(X)+\delta Y(X)$, where $|\delta Y| \ll |Y|$,

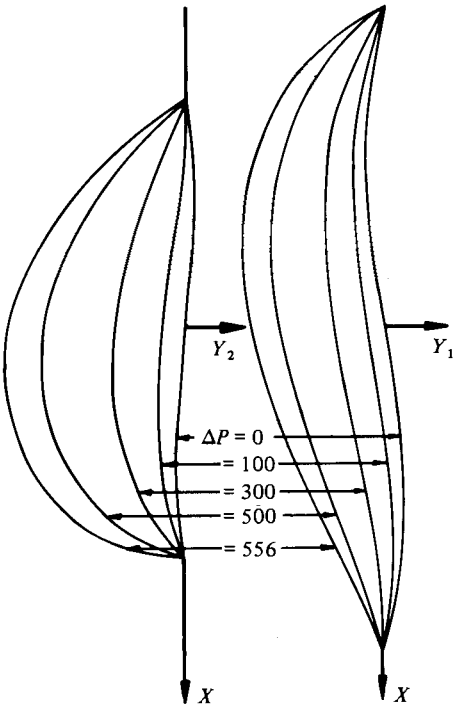

FIGURE 4. Effect of a differential pressure drop, ΔP (N m^{-2}), on the distortion of a two-sided vertical weld pool.

and we assume that the ends remain fixed, i.e. $\delta Y = 0$ at $X = \pm \frac{1}{2}$. The corresponding change in energy is

$$\delta E = \int_{-\frac{1}{2}}^{\frac{1}{2}} \{[1+(Y'+\delta Y')^2]^{\frac{1}{2}} - [1+Y'^2]^{\frac{1}{2}} - \epsilon X \delta Y\} dX.$$

From the Euler–Lagrange equation (Craggs 1973), terms of order δY vanish identically and we have

$$\delta E = \frac{1}{2}\int_{-\frac{1}{2}}^{\frac{1}{2}} \delta Y'^2 (1+Y'^2)^{-\frac{3}{2}} dX + O(\delta Y'^3). \tag{21}$$

Provided $\delta Y'$ is small, the first term on the right-hand side dominates and δE is positive definite. Hence our equilibrium profile is stable for small two-dimensional disturbances provided the molten material remains attached to the corners.

The small region of slightly overhanging profiles corresponding to the segment BC in figure 3 is also stable. To prove the stability requires a rather lengthy argument and we shall give only a very brief outline of the proof here. As the profile is overhanging, we must first write down the energy integral E in parametric form. The most convenient form for the parameter t is to take $t = X$ in the range $0 < X < \frac{1}{2}$ and $t = B - Y$ in the range $X > \frac{1}{2}$, where the constant B is chosen to make t continuous at the join $X = \frac{1}{2}$. The other half of the curve is parametrized in the same way. We may now write down the second variation of the energy, taking care at the join $X = \frac{1}{2}$, where the perturbations are not defined continuously in terms of the parameter t. Finally an argument

similar to Jacobi's second condition shows that the second variation will be positive definite and the equilibrium will be stable provided the solution of a pair of ordinary differential equations does not possess a zero within the range of interest. Numerical tests show that this is the case throughout the range BC. If we apply the same test to points in the segment CD, we find that the solution of the pair of ordinary differential equations does possess a zero so that the energy is no longer positive definite and the segment CD corresponds to a region of unstable equilibrium.

The stability of the problem of § 2.2 is similar. For a problem with both profiles single-valued the energy per unit length is now

$$E = \int_{-\frac{1}{2}}^{\frac{1}{2}} \{(1+Y_1'^2)^{\frac{1}{2}} - \epsilon XY_1 + \Delta PY_1\}\,dX + \int_{-\frac{1}{2}\lambda}^{\frac{1}{2}\lambda} \{(1+Y_2'^2)^{\frac{1}{2}} + \epsilon XY_2\}\,dX$$

to within an arbitrary constant. We suppose now that the two surfaces are slightly distorted to $Y_1+\delta Y_1$ and $Y_2+\delta Y_2$ and we again assume that we have attachment at the corners. The change in energy is now

$$\delta E = \int_{-\frac{1}{2}}^{\frac{1}{2}} \tfrac{1}{2}(1+Y_1'^2)^{-\frac{3}{2}}\delta Y_1'^2\,dX + \int_{-\frac{1}{2}\lambda}^{\frac{1}{2}\lambda} \tfrac{1}{2}(1+Y_2'^2)^{-\frac{3}{2}}\delta Y_2'^2\,dX + O(\delta Y_1'^3+\delta Y_1'^3), \tag{22}$$

where the terms of $O(\delta Y_1)$ and $O(\delta Y_2)$ have vanished because of the equilibrium equations (12) and (13). The second-order terms will dominate provided $\delta Y_1'$ and $\delta Y_1'$ are sufficiently small, so that δE is positive definite and our single-valued equilibrium profiles are stable to small two-dimensional disturbances.

We do not consider the stability of overhanging profiles here, but we expect this to follow along similar lines to the one-sided problem.

3. Horizontal plate

3.1. *Two-dimensional slot*

We now consider a horizontal plate. The interesting case occurs when both the upper and lower surfaces are molten. Consider firstly an infinitely long slot with top and bottom widths L_1 and L_2, and thickness h. The equations for the unknown top and bottom surfaces $Y_1(X)$ and $Y_2(X)$ are

$$\{Y_1'/(1+Y'^2)^{\frac{1}{2}}\}' = \epsilon(Y_1-C) \tag{23}$$

and

$$-\{Y_2'/(1+Y_2'^2)^{\frac{1}{2}}\}' = \epsilon(Y_2-C), \tag{24}$$

the normalization being the same as in (14). The boundary conditions are

$$Y_1 = 0 \quad \text{at} \quad X = \pm\tfrac{1}{2}, \tag{25}$$

$$Y_2 = -H \quad \text{at} \quad X = \pm\tfrac{1}{2}\lambda, \tag{26}$$

where $H = h/L_1$ and mass conservation implies that

$$\int_0^{\frac{1}{2}} Y_1\,dX = \int_0^{\frac{1}{2}\lambda} (Y_2+H)\,dX, \tag{27}$$

noting that the profiles must be symmetric about $X = 0$. In this case the effect of a differential pressure, Δp, can be incorporated by simply increasing H by an amount $\Delta p/\rho g L_1$. The solution of the linearized problem (with $Y_1'^2 \ll 1$ and $Y_2'^2 \ll 1$) is straightforward and given by

$$Y_1 = H(1-\cosh \epsilon^{\frac{1}{2}} X/\cosh \tfrac{1}{2}\epsilon^{\frac{1}{2}})/(\nu-1), \tag{28}$$

$$Y_2 = H(1-\nu \cos \epsilon^{\frac{1}{2}} X/\cos \tfrac{1}{2}\lambda\epsilon^{\frac{1}{2}})/(\nu-1), \tag{29}$$

where

$$\nu = (1-(2/\epsilon^{\frac{1}{2}})\tanh \tfrac{1}{2}\epsilon^{\frac{1}{2}})/(\lambda-(2/\epsilon^{\frac{1}{2}})\tan \tfrac{1}{2}\lambda\epsilon^{\frac{1}{2}}). \tag{30}$$

Obviously, this linearized solution is adequate only if the distortion of the surfaces is small. The linearized solution breaks down altogether when $\nu = 1$ and by inspection of (30) we note that the first positive real root of $\nu = 1$ occurs in the range $\pi < \epsilon^{\frac{1}{2}}\lambda < 3\pi$.

In general we must solve the nonlinear problem, and integrating (23) and (24) yields

$$(1+Y_1'^2)^{-\frac{1}{2}} = 1-\tfrac{1}{2}\epsilon\{(Y_1-C)^2-(Y_1^*-C)^2\} \equiv A_1(Y_1) \quad \text{say}, \tag{31}$$

and

$$(1+Y_2'^2)^{-\frac{1}{2}} = 1+\tfrac{1}{2}\epsilon\{(Y_2-C)^2-(Y_2^*-C)^2\} \equiv A_2(Y_2) \quad \text{say}, \tag{32}$$

where Y_1^* and Y_2^* are the values of Y_1 and Y_2 at the centre $X = 0$, both of which are unknown at this stage. Rearranging equation (31), integrating and using the boundary condition (25) gives

$$\int_{Y_1^*}^{0} A_1(1-A_1^2)^{-\frac{1}{2}}\,dY_1 - \tfrac{1}{2} = 0, \tag{33}$$

which may also be reduced to elliptic integrals. Equation (32) may be treated in a similar way. Integrating the mass conservation condition (27) by parts as before gives

$$\{1-A_1^2(0)\}^{\frac{1}{2}} + \{1-A_2^2(-H)\}^{\frac{1}{2}} - \tfrac{1}{2}\epsilon\{H\lambda - C(1-\lambda)\} = 0, \tag{34}$$

and (32)–(34) are three equations which may be solved to determine C, Y_1^* and Y_2^*.

Figure 5 shows the development of the sag with increasing differential pressure, taking $\epsilon = 3$ and $\lambda = 0{\cdot}6$. From figure 5 we see that the lower surface is nearly vertical at the corner for $H = 1{\cdot}5$ and, from a practical point of view, this weld would be unacceptable. Another extreme arises when the upper surface becomes vertical at the corner, e.g. when heating a horizontal plate from underneath so that $\lambda > 1$.

Finally, we note that, if $C < -H$, then the lower surface has a point of inflexion. Furthermore, by inspection of the form of equation (24) we see that Y_2' is symmetric about the point of inflexion. In fact, $Y_2' = 0$ when $Y_2 = Y_2^*$ and $Y_2 = 2C - Y_2^*$, corresponding to a minimum and a maximum, respectively. Clearly the most extreme profile occurs when the maximum coincides with the bottom corner (i.e. at $Y_2 = -H$) in which case $C = -\frac{1}{2}(H - Y_2^*)$. For this value of C the point of inflexion arises at the mid-point of the lower boundary on and we may assert that no equilibrium profiles exist for more negative values of C. Hence, this case presents another extreme to the types of welding profiles that can be obtained.

Figure 5 also shows a profile with the *lower* boundary vertical at the corner. Figure 6 shows a profile with the *upper* boundary vertical at the corner. Figure 7 is a case

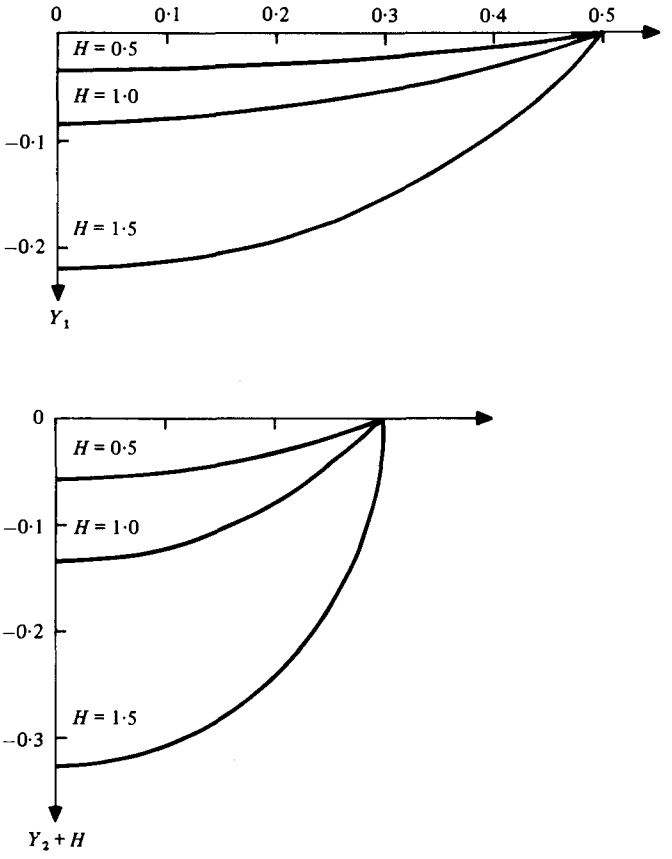

FIGURE 5. Weld-pool sag for a horizontal plate with increasing differential pressure; $\epsilon = 3$, $\lambda = 0{\cdot}6$.

where the point of inflexion is very close to the mid-point of the lower surface. However, it is possible to vary both ϵ and H significantly, remaining extremely close to this limit, but the results do not indicate that the limit can actually be achieved.

3.2. *Stability for a horizontal slot*

We again restrict our attention to disturbances which leave the problem two-dimensional and we exclude values of ϵ and H which lie on or to the right of the critical curve as in figure 9. To within an arbitrary constant the total potential energy per unit length is

$$E = \int_{-\frac{1}{2}}^{\frac{1}{2}} \{(1+Y_1'^2)^{\frac{1}{2}} + \tfrac{1}{2}\epsilon Y_1^2\}\, dX + \int_{-\frac{1}{2}\lambda}^{\frac{1}{2}\lambda} \{(1+Y_2'^2)^{\frac{1}{2}} - \tfrac{1}{2}\epsilon Y_2^2\}\, dX. \tag{35}$$

We now consider the surfaces to be displaced from their equilibrium shapes $Y_1(X), Y_2(X)$ to the perturbed shapes $Y_1+\xi_1$, $Y_2+\xi_2$. The values ξ_1 and ξ_2 must be zero at the corners and mass conservation implies that

$$\int_{-\frac{1}{2}}^{\frac{1}{2}} \xi_1\, dX - \int_{-\frac{1}{2}\lambda}^{\frac{1}{2}\lambda} \xi_2\, dX = 0. \tag{36}$$

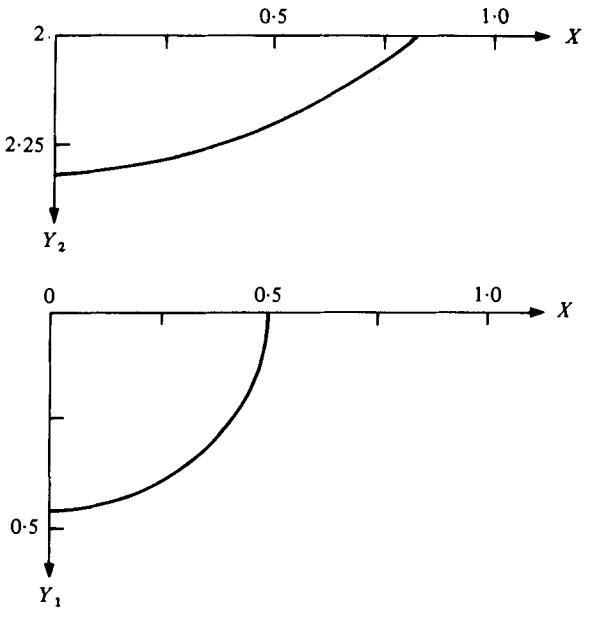

FIGURE 6. Weld-pool sag in a horizontal plate showing the upper boundary vertical at the corner; $\epsilon = 1{\cdot}473$, $\lambda = 1{\cdot}66$, $H = 2$.

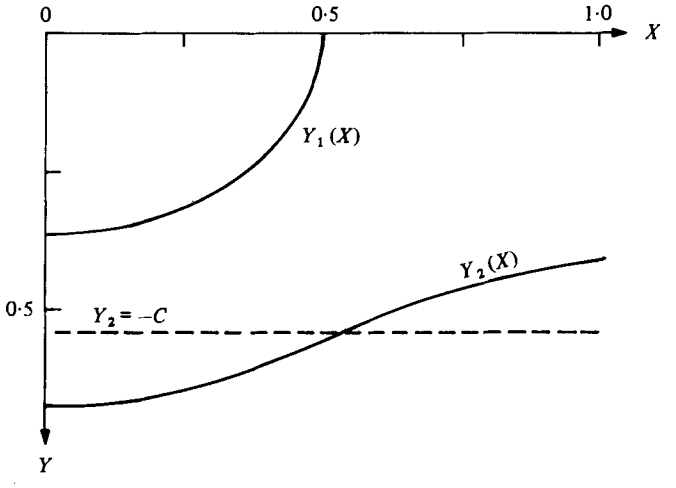

FIGURE 7. Weld-pool sag in a horizontal plate showing a point of inflexion of the lower surface.

Substituting in (35), using (36) and the equilibrium equations (23) and (24), we obtain the change in potential energy as

$$\delta E = \delta E_1 + \delta E_2,$$

where

$$\delta E_1 = \frac{1}{2}\int_{-}^{\frac{1}{2}} \{(1+Y_1'^2)^{-\frac{3}{2}}\xi_1'^2 + \epsilon\xi_1^2\}\,dX \tag{37}$$

and

$$\delta E_2 = \frac{1}{2}\int_{-\frac{1}{2}\lambda}^{\frac{1}{2}\lambda} \{(1+Y_2'^2)^{-\frac{3}{2}}\xi_2'^2 - \epsilon\xi_2^2\}\,dX. \tag{38}$$

We note that δE_1 is positive definite and stability clearly holds if δE_2 is also positive definite. We first derive a sufficient condition for this to be true.

Let us assume that $\partial Y_2(X;C)/\partial C \leqslant 0$ for $-\frac{1}{2}\lambda \leqslant x \leqslant \frac{1}{2}\lambda$. To evaluate $\partial Y_2/\partial C$ we solve the equilibrium equation (24) with the boundary conditions (26) but we relax the constraint of mass conservation (27). It is then possible to determine the value of $\partial Y_2/\partial C$ for the equilibrium value of C.

Defining $\eta = \partial Y_2/\partial C - 1$, so that $\eta < 0$ everywhere, we see that η satisfies

$$\{(1+Y_2'^2)^{-\frac{3}{2}}\eta'\}' + \epsilon\eta = 0 \tag{39}$$

(by differentiating (24) with respect to C). We now introduce a function $U(X)$ which satisfies equation (39) and the initial conditions $U = 0$, $U' = 1$ at $X = -\frac{1}{2}\lambda$. Since the zeros of two linearly independent solutions of this type of equation interlace (Burkill 1962), U can have at most one zero in the interval $-\frac{1}{2}\lambda \leqslant X \leqslant \frac{1}{2}\lambda$. Hence $U > 0$ for $X > -\frac{1}{2}\lambda$ and we divide throughout by U, obtaining

$$\epsilon = -\{(1+Y_2'^2)^{-\frac{3}{2}}U'\}'/U.$$

Following Craggs (1973), we can avoid considering the form of Y_2 by substituting for ϵ in (38) and integrating by parts to obtain

$$\begin{aligned}\delta E_2 &= \frac{1}{2}\int_{-\frac{1}{2}\lambda}^{\frac{1}{2}\lambda} (1+Y_2'^2)^{-\frac{3}{2}}(\xi_2' - \xi_2 U'/U)^2\,dX \\ &\geqslant 0,\end{aligned}$$

where we have assumed that ξ_2' is finite at $X = -\frac{1}{2}\lambda$ so that

$$\lim_{X\to-\frac{1}{2}\lambda} (\xi_2^2/U) = 0.$$

For the extreme $\delta E_2 = 0$ we require $\xi_2' - \xi_2 U'/U \equiv 0$, i.e. $\xi_2 = AU$. But $U(\frac{1}{2}\lambda) > 0$ and $\xi_2(\frac{1}{2}\lambda) = 0$, so $A = 0$ and $\xi_2 \equiv 0$. Hence δE_2 is positive definite and the condition

$$\partial Y_2/\partial C \leqslant 0 \tag{40}$$

is sufficient for stable equilibrium. This condition is equivalent to a stability criterion found by Majumdar & Michael (1976) for the stability of a drop hanging from a tap under constant pressure.

If we go outside this region where stability has been demonstrated, the situation is not so clear. We can no longer expect δE_2 to be positive definite, i.e. we expect to be able to find a perturbation ξ_2 for which $\delta E_2 < 0$. However in general $\int \xi_2\,dX \neq 0$ and hence by mass conservation $\int \xi_1\,dX$ is also non-zero. Since δE_1 is positive definite it is possible that the sum $\delta E_1 + \delta E_2$ may also be positive definite, which would mean that the presence of the upper surface would actually extend the region of stable equilibrium. We do not attempt to analyse such a stability problem in this paper.

It is a straightforward numerical exercise to determine the values of the parameters ϵ, H and λ at which $\partial Y_2/\partial C$ changes sign, which marks the limit for which stability has been demonstrated. Figures 8 and 9 show the variation of H with ϵ for this stability criterion to be satisfied for the cases $\lambda = \frac{3}{5}$ and $\frac{5}{3}$ respectively. Figure 8 also shows a

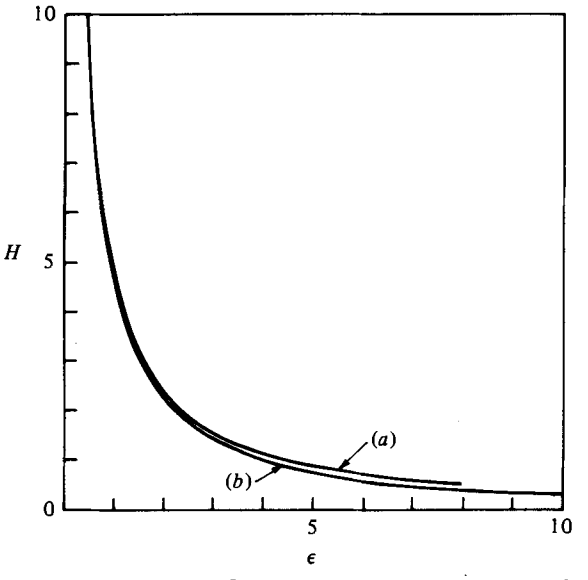

FIGURE 8. Variation of H with ϵ for $\lambda = \frac{8}{5}$ for (*a*) the limiting case with the lower surface vertical at the corner, (*b*) the stability criterion (40).

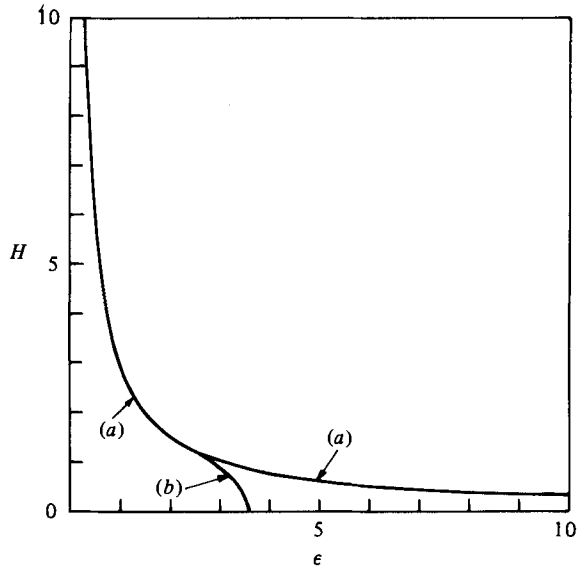

FIGURE 9. Variation of H with ϵ for $\lambda = \frac{8}{5}$ for (*a*) the limiting case with the upper surface vertical at the corner, (*b*) the stability criterion (40).

curve on which the lower surface becomes vertical at the corner. This curve is truncated at around $\epsilon = 8$. For larger values of ϵ a point of inflexion appears in the lower surface (i.e. $C < -H$) and the limit to our analysis arises when the lower surface becomes vertical at the point of inflexion rather than at the corner. We do not consider this case. For the range of parameters covered we note that the stability curve lies below the limit with the vertical corner at the lower surface. Figure 9 also shows the

curve on which the upper surface becomes vertical at a corner. We note that this curve intersects the stability curve at $\epsilon = 2{\cdot}404$; $H = 1{\cdot}125$ and, for larger values of ϵ, the stability curve lies below the vertical corner curve. Indeed the stability curve intersects the line $H = 0$ at $\epsilon = 3{\cdot}55$. For $\epsilon < 2{\cdot}404$ the stability curve would lie above the curve a, so that for $\lambda = \frac{5}{3}$, $\epsilon < 2{\cdot}404$ we can assert that all the monotonic profiles are stable.

4. Discussion

Our model considers the distortion of the weld profile due to the hydrostatic pressure in the liquid metal. However the real welding situation has several complicating features which we have not considered. We have assumed that the fluid is stationary, but in practice it is observed to be in motion due to electromagnetic $\mathbf{j} \times \mathbf{B}$ forces in the liquid metal (Woods & Milner 1971). Atthey (1980) has estimated the pressure distribution arising from these $\mathbf{j} \times \mathbf{B}$ forces to be around 25 N m^{-2} for a Gaussian current input from the arc, taking a current of 100 A and a characteristic arc radius of 2·5 mm. This compares with a typical hydrostatic pressure of 250 N m^{-2}. However, for more concentrated distributions, this effect could become very important. Another effect is the external pressure over the two surfaces. The pressure drop is caused primarily by the interaction of the electric arc and the jet of shielding gas with the liquid surface and its value may be expected to vary across the surface. To measure this variation with position would be extremely difficult and even an average value is relatively hard to obtain.

There is also some uncertainty in the value of the surface-tension coefficient, T. We can expect the value of T to vary with temperature, which in turn will vary across the surface. The presence of slag on the metal surface and the possibility of oxidation may also affect T. Furthermore the assumption of volume conservation of material should be adjusted to allow for thermal expansion; post-mortem examination of weld sections indicates the increase in volume to be around 5–10 %.

Figures 10(a, b, d) show actual sections of etched welds, obtained by Meewezen (1976, private communication). Figure 10(c) shows the profile given by our analysis for a two-dimensional slot of the same dimensions ($L_1 = 7{\cdot}49$ mm, $L_2 = 5{\cdot}22$ mm) by taking $T = 1$ N m^{-1} and $\rho = 7800$ kg m^{-3}, and assuming a pressure drop $\Delta P = 200$ N m^{-2}. This value of ΔP was chosen so as to give good agreement with the experimental results. A pressure drop of $\Delta P = 200$ N m^{-2} is of the same order as that measured experimentally by Erokhin, Bukarov & Ischenko (1971) for a TIG (Tungsten-Inert-Gas) arc with a current of 100 A, using a water-cooled copper workpiece. Unfortunately the same authors also showed that the pressure varied by at least a factor of 2 owing to the electrode shape, and it is possible that there could be significant differences between a copper workpiece and a real weld pool with metal vapour in the welding arc. Hence we can only expect qualitative agreement with experimental results and a proper test of the analysis would require measurement of arc pressure together with weld-pool sag under carefully controlled conditions. The qualitative similarity is encouraging, though close agreement is hardly to be expected in view of the limitations in the model discussed above.

Finally, we consider the question of whether the shape of the boundary remains unchanged during the process of solidification. For the one-sided problem we can

show that this is likely to be the case by considering a small amount of solidification so that the pool now occupies a region $-\frac{1}{2}+\delta \leqslant X \leqslant \frac{1}{2}-\delta$. The remaining surface automatically satisfies equation (5) and, in order that the liquid attaches at the 'new' corners, we expect $Y(-\frac{1}{2}+\delta)$ and $Y(\frac{1}{2}-\delta)$ to be equal to their old values when the pool extended from $-\frac{1}{2} \leqslant X \leqslant \frac{1}{2}$. One solution which satisfies these conditions together with the mass conservation condition (in an appropriately modified form) is the original solution and, although we have not considered the question of uniqueness, we intuitively expect this solution to still apply. In the above argument we have of course assumed that the solid and liquid metal have the same density.

A further complication arises with the two-sided problem. When no pressure drop is applied ($\Delta P = 0$), the problem decouples to two separate one-sided problems and the above argument will apply. On the other hand, when $\Delta P \neq 0$ the pressure drop will act on proportionally different areas as the two surfaces solidify and it is not immediately clear whether or not this will affect the shapes of the remaining liquid surfaces. However, we note that equations (12) and (13) with the conservation condition (15) are equivalent to the formulation

$$\{Y_1'(1+Y_1'^2)^{-\frac{1}{2}}\}' = -\epsilon(X-C_1), \tag{41}$$

$$\{Y_2'(1+Y_2'^2)^{-\frac{1}{2}}\}' = \epsilon(X-C_2), \tag{42}$$

$$\int_{-\frac{1}{2}}^{\frac{1}{2}} Y_1 dX = I_0, \tag{43}$$

$$\int_{-\frac{1}{2}\lambda}^{\frac{1}{2}\lambda} Y_2 dX = I_0, \tag{44}$$

where I_0 is chosen so that

$$\epsilon(C_1-C_2) = \Delta P. \tag{45}$$

Thus the only effect of the pressure drop is to determine the excess volume of each profile (I_0) through equation (45). Again the problem has decoupled into two one-sided profiles and, by an argument similar to that for the one-sided case, we may show that the liquid profiles are frozen with no change.

REFERENCES

Atthey, D. R. 1980 *J. Fluid Mech.* **98**, 787.

Burkill, J. C. 1962 *Theory of Ordinary Differential Equations*. Edinburgh: Oliver and Boyd.

Craggs, J. W. 1973 *Calculus of Variations*. London: George Allen and Unwin.

Erokhin, A. A., Bukarov, V. A. & Ischenko, Yu. S. 1971 *Weld Prod.* (*U.S.S.R.*) **18** (12), 25.

Majumdar, S. R. & Michael, D. H. 1976 *Proc. Roy. Soc.* A **351**, 89.

Nishiguchi, K., Ohji, T. & Matsui, H. 1977 *IIW Doc.* 212-391-77.

Padday, J. F. 1971 *Phil. Trans. Roy. Soc.* A **269**, 265.

Padday, J. F. & Pitt, A. R. 1973 *Phil. Trans. Roy. Soc.* A **275**, 489.

Pitts, E. 1973 *J. Fluid Mech.* **59**, 753.

Pitts, E. 1974 *J. Fluid Mech.* **63**, 487.

Pitts, E. 1976 *J. Fluid Mech.* **76**, 641.

Woods, R. A. & Milner, D. R. 1971 *Weld. J. Res. Suppl.* **50**, 163s.

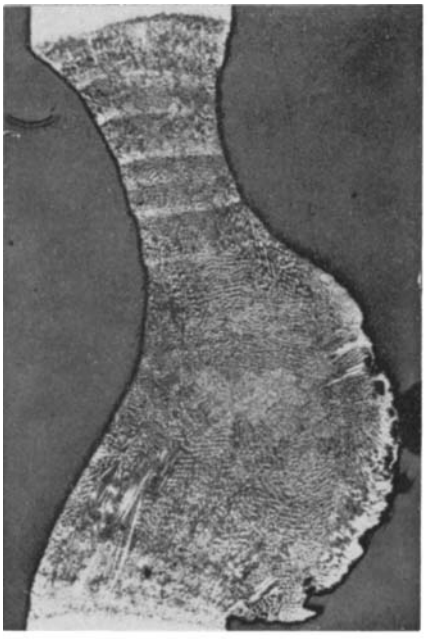

(*a*)

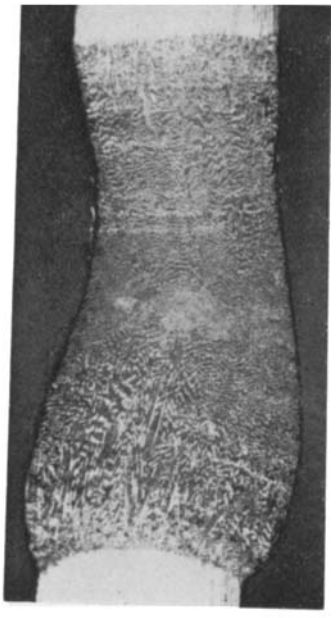

(*d*)

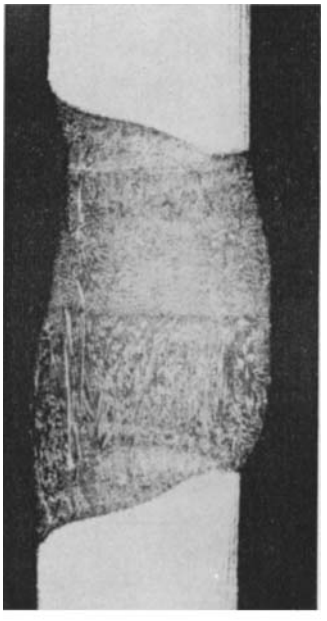

(*b*)

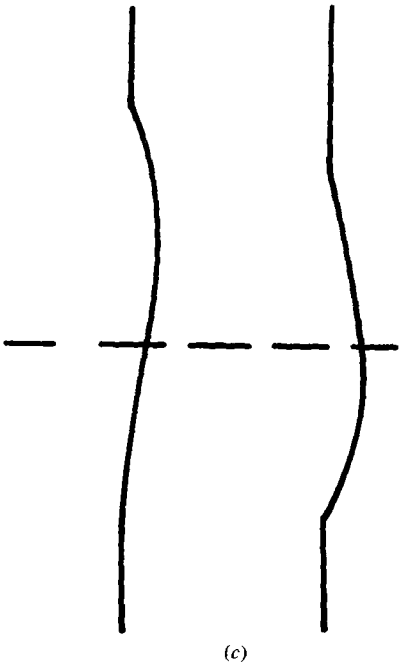

(*c*)

FIGURE 10. Actual and computed two-sided vertical weld profiles.